Pak. J. Bot., 55(3): 1023-1034, 2023. DOI: http://dx.doi.org/10.30848/PJB2023-3(21)

TRANSCRIPTOME ANALYSIS OF *LYCORIS RADIATA* BULB TIPS AT DIFFERENT DEVELOPMENTAL STAGES

XUERU JIANG[1#], XUYING WEI[#], HUITING CHEN[1], YAO ZHANG[1], MEIXIA MA[1] AND JUNHUO CAI[1*]

[1]*College of Landscape and Art, Jiangxi Agricultural University, Nanchang 330045, P.R. China*
[2]*College of Art, Jiangxi Finance and Economics University, Nanchang 330032, P.R. China*
[*]*Corresponding author's email: Cjhuo7692@163.com*
[#]*Contributed equally to this work*

Abstract

Lycoris radiata (L'Herit.) Herb is a commonly used medicinal-ornamental herb in China, and its growth rhythm is characterized as "flowers and leaves not meeting." In this research, transcriptomic analyses of *L. radiata* bulb tips were conducted at six developmental stages, specifically: LO (leafing out), RLE (rapid leaf extension), LMa (leaf maturity), LWi (leaf withering), Dor (dormancy), and Flo (flowering), to identify the differentially expressed genes (DEGs). There were 6,157 DEGs in RLE vs. LO, 18,193 in LMa vs. RLE, 4,362 in LWi vs. LMa, 5,800 in Dor vs. LWi and 7,373 in Flo vs. Dor. The KEGG pathways 'hormone signal transduction' and 'starch and sucrose metabolism' and the biological processes 'carbohydrate metabolism' and 'stress response' were significantly enriched by upregulated DEGs in LMa vs. RLE during leaf development. KEGG pathways of 'biosynthesis of amino acids,' 'circadian rhythm – plant,' and 'gap junction' were significantly enriched by upregulated DEGs in LWi vs. LMa, Dor vs. LWi, and Flo vs. Dor, respectively, during floral differentiation and flowering. Weighted gene coexpression network analysis (WGCNA) showed that genes encoding ribosomal proteins were identified as hub genes in both the RLE and Flo stages, and genes encoding 16.0 kDa heat shock protein and heat stress transcription Factor C-2a-like were respectively identified as RLE and LWi stage-specific hub genes. Together, these analyses provide a valuable reference for studying the molecular mechanism of *L. radiata* growth rhythm from the aspects of temperature adaptability, sugar signal transduction, sugar metabolism, and circadian rhythm.

Key words: Differentially expressed genes (DEGs), Floral differentiation, Leaf development, KEGG pathways, Growth rhythm.

Introduction

Lycoris radiata is widely distributed in southwest China, Japan, and South Korea. It has rich natural germplasm resources in China (Wang, 1990; Zhang *et al*., 2015). The plant has large business prospects and market development potential due to its high medicinal and ornamental value. In recent years, the market demand and planting area of *L. radiata* have increased rapidly. Unlike most bulbous flowers, the growth rhythm of *Lycoris* is characterized by "flowers and leaves not meeting" (Kawano, 2009). Its leaves sprout after flowering in autumn, grow vigorously in autumn and winter, and wither in summer. Following summer, *Lycoris* enters the dormancy period, and then scapes and blossoms, thus ending a growth cycle (Yang, 2009). Understanding the physiological and molecular regulation mechanism of this unique growth rhythm may provide a theoretical basis for studying *Lycoris* cultivation technology.

Cai *et al*., (2019, 2020) divided the growth and development of *L. radiata* into 6 stages, including: leafing out (LO) in October, rapid leaf extension (RLE) in November, leaf maturity (LMa) from December to February, leaf withering (LWi) from March to May, dormancy (Dor) from June to July and flowering (Flo) from August to October. Furthermore, the changes in organ biomass in different developmental periods were also studied. Bulbs are used as nutrient "sources" in reproductive and vegetative growth stages, while in the later stage of leaf growth, they are used as storage materials.

The activities of superoxide dismutase (SOD) and peroxidase (POD) and the content of soluble sugar were decreased in bulbs during the dormancy stage but increased during the flowering stage (Cai *et al*., 2018a, 2019). A high content of indole-acetic acid (IAA) and a low content of abscisic acid (ABA) and gibberellin (GA) in bulbs was conducive to the morphological differentiation of flower buds, while a relatively high content of GA was conducive to the morphogenesis and sprouting of flower organs of *L. radiata* (Cai, 2012; Zhang *et al*., 2019a). On the other hand, the leaf growth, scaping, and flowering of *L. radiata* are affected by environmental temperature. High temperatures (>25°C) are not conducive to leaf growth but are beneficial to scaping and flowering (Cai *et al*., 2018b).

As mentioned above, the physiological mechanism of the *L. radiata* growth rhythm has been fully studied, but its molecular mechanism remains unknown. Although transcriptome and metabolic analyses have been used to study galantamine biosynthesis (Park *et al*., 2019), changes in hormone biosynthesis and carbohydrate metabolism in *Lycoris* bulblet initiation (Xu *et al*., 2020a), they have not been used to study *L. radiata* development and flowering. In this study, RNA-seq technology was used to analyse the transcriptomes of the bulb tips at different developmental stages of *L. radiata*. The differentially expressed genes (DEGs) with key roles and the modules of coexpressed genes expressed predominantly at specific stages of *L. radiata* development were identified. This study provides insights into the molecular mechanisms underlying *L. radiata* development and flowering.

Materials and Methods

Plant materials: Bulbs of *L. radiata* with a diameter of 3 ± 0.1 cm were planted outdoors in the Jiangxi Agricultural University Flower Gardens (28°76′ N, 115°83′ E) in the fall of 2018. The soil type is red soil

derived from quaternary red clay with a pH of 6.43. The planting area is in a subtropical monsoon climate zone. The average minimum temperature occurs in January, which is 3.9℃, and the average maximum temperature occurs in July, which is 38.7℃. The bulbs of *L. radiata* were sampled in the morning (approximately 9 a.m.) of October 9 (during the LO stage), October 27 (during the RLE stage), December 30 (during the LMa stage), April 13 (during the LWi stage), June 28 (during the Dor stage), and September 3 (during the Flo stage), including samples from 45 plants each time (Jiang *et al*., 2021). Then, all bulbs were taken into the lab, washed with distilled water, and cut open to obtain bulb tips in a cold chamber at 4°C. The weather was stable within three days before and after the sampling date. The resulting bulb tips were immediately placed in liquid nitrogen and then stored in a -80°C refrigerator for subsequent experimental analysis. In the experiment, each sample was repeated three times, and each repetition contained 15 bulb tips.

RNA extraction and sequencing: Approximately 0.2 g bulb tips were ground into powder in a mortar with liquid nitrogen. Total RNA from three replicates was extracted independently using Invitrogen's TRIzol reagent (Carlsbad, CA, USA) in accordance with the instructions. Then, 1% agarose gel electrophoresis was used to monitor RNA degradation and contamination. A NanoPhotometer® spectrophotometer (IMPLEN, CA, USA) and an RNANano 6000 Assay Kit for the Agilent Bioanalyzer 2100 system (Agilent Technologies, CA, USA) were used to assess the purity and integrity of the RNA. RNA samples were sent to Applied Protein Technology Co., Ltd. (Shanghai, China) for sequencing.

Assembly and annotation: By removing low-quality reads and reads containing adapters and poly-N from the raw data, high-quality clean reads were obtained for downstream analyses. Transcriptome assembly was completed based on the left.fq and right.fq by Trinity (Grabherr *et al*., 2011). The longest transcript was selected as the unigene of the gene. All transcripts and unigenes were counted, and the subsequent bioinformatics analysis was conducted on this basis. Furthermore, all unigenes were annotated based on the following public databases: NCBI nonredundant protein sequences (Nr), NCBI nonredundant nucleotide sequences (Nt), Clusters of Orthologous Groups of proteins (KOG/COG), and Gene Ontology (GO).

Differential expression analysis: DEG analysis between adjacent developmental stages was conducted by the DESeq R package (1.10.1) (Wang *et al*., 2010). The P values adjusted by Benjamini and Hochberg's approach (Q value) (Benjamini & Hochberg, 1995) were used to control the false discovery rate (FDR). When the Q value <0.05 and the absolute value Log2 (fold change, FC)>1, the gene was called a differentially expressed gene (Anders & Huber, 2012).

The DEGs identified in the above steps were analysed for GO enrichment in the Gene Ontology (GO) database (Young *et al*., 2010) and annotated in the KEGG (Kyoto Encyclopedia of Genes and Genomes, http://www.genome.jp/kegg/) database to identify the pathway in which the DEGs were located (Mao *et al*., 2005). For both GO and KEGG pathway enrichment, a Q value<0.05 was used as the threshold of significant enrichment. Moreover, the R package WGCNA (weighted gene coexpression network analysis, https://cran.r project.org/web/packages/WGCNA/index.html) was applied to perform the coexpression network analysis (Langfelder & Horvath, 2008).

Results

Sequencing data quality: After trimming and applying the quality filter, the clean read number of the individually sequenced libraries ranged from 39,366,080 to 59,882,636, and the clean bases ranged from 5.47G to 8.32G (Table 1). The Phred quality score (Q score) is usually used to evaluate the accuracy of a sequencing platform. In this study, the minimum percentage of bases with Q scores greater than 20 ($Q \geq 20$) and 30 ($Q \geq 30$) for the individually sequenced libraries was 98.05% and 94.03%, respectively. This showed that the high-quality clean reads obtained can be used for subsequent analysis.

DEGs identification between the adjacent developmental stages: Pairwise comparison at the adjacent developmental stages of *L. radiata* was conducted to identify the genes correlating with development. With the development of leaves (from the LO stage to LMa), the number of DEGs identified between adjacent developmental stages increased (Fig. 1). Most DEGs were identified between LMa and RLE (18,193). Similarly, with leaf senescence and flower bud development (from the LWi to Flo stages), the number of DEGs identified between adjacent stages also increased (Fig. 1). For example, there were 4,362 DEGs identified between LWi vs. LMa, but 7,373 DEGs identified between Flo vs. Dor.

GO enrichment analysis of the DEGs: GO enrichment analysis of DEGs was conducted and the DEGs identified in each comparison group were divided into three categories: biological processes (BP), cellular components (CC), and molecular functions (MF) (Table 2). The top 5 significantly enriched GO terms of upregulated and downregulated DEGs in the biological process category are listed in Figs. 2 and 3.

For the three stages of leaf development (LO, RLE, and LMa), the upregulated DEGs of LMa vs. RLE enriched the most GO terms at a Q value <0.05, followed by RLE vs. LO (Table 2). There were 25 upregulated GO terms mapped to biological processes in LMa vs. RLE, including 'response to stimulus' (117), 'carbohydrate metabolic process' (55), and 'response to abiotic stimulus' (24), etc. (Fig. 2). Some upregulated DEGs involved in 'carbohydrate metabolic process' are shown in Table 3. Among these, the expression levels of genes annotated as glyceraldehyde-3-phosphate dehydrogenase-2C cytosolic (GAPC2), fructan 6G-fructosyltransferase (6G-FFT), and beta-amylase 8 (BAM8)-like protein were all increased more than 128-fold (log2FC >7) in LMa relative to RLE. In addition, there were 24 upregulated DEGs in LMa vs. RLE involved in 'response to abiotic stimulus', including genes encoding protein ESKIMO 1 (Log2FC= 6.65), glyceraldehyde-3-phosphate dehydrogenase GAPA1, chloroplastic isoform X1 (Log2FC= 6.38), and HSP20-like chaperones superfamily protein (Log2FC=5.33) (Table 3).

Table 1. Summary of Illumina transcriptome sequencing.

Sample	Raw_reads	Clean_reads	Clean_bases	Error rate (%)	Q20 (%)	Q30 (%)	GC (%)
LO_1	46,949,372	46,789,430	6.5G	0.02	98.30	94.57	48.43
LO_2	50,530,454	50,311,898	6.95G	0.02	98.40	94.89	47.56
LO_3	47,557,842	47,328,360	6.58G	0.02	98.30	94.67	47.33
RLE_1	60,127,732	59,882,636	8.32G	0.02	98.42	94.94	48.07
RLE_2	46,255,014	46,092,948	6.4G	0.02	98.49	95.12	47.84
RLE_3	48,691,088	48,505,958	6.72G	0.02	98.40	94.92	47.95
LMa_1	47,133,982	46,979,722	6.52G	0.02	98.40	94.86	46.08
LMa_2	41,427,216	41,260,906	5.73G	0.02	98.29	94.61	46.09
LMa_3	46,770,282	46,604,204	6.44G	0.02	98.41	94.91	46.2
LWi_1	43,229,864	43,087,526	5.98G	0.02	98.37	94.73	47.89
LWi_2	50,995,890	50,799,380	7.07G	0.02	98.42	94.89	47.6
LWi_3	47,326,832	46,609,110	6.45G	0.02	98.37	94.78	48.25
Dor_1	49,255,808	48,999,096	6.79G	0.03	98.05	94.03	47.64
Dor_2	45,690,260	45,474,530	6.32G	0.02	98.22	94.49	46.64
Dor_3	48,065,536	47,869,366	6.65G	0.02	98.32	94.67	47.13
Flo_1	39,517,852	39,366,080	5.47G	0.02	98.41	94.94	47.13
Flo_2	40,496,724	40,296,902	5.6G	0.02	98.12	94.22	47.69
Flo_3	42,316,850	42,125,508	5.85G	0.02	98.22	94.46	48.55

Q20 (%) and Q30 (%), percentage of bases with a Phred quality score (Q score) greater than 20 and 30, respectively. GC (%), the percentage of G and C bases in all clean reads. LO represents the stage of leafing out; RLE represents the stage of rapid leaf extension; LMa represents the stage of leaf maturity; LWi represents the stage of leaf withering; Dor represents the stage of dormancy; and Flo represents the stage of flowering

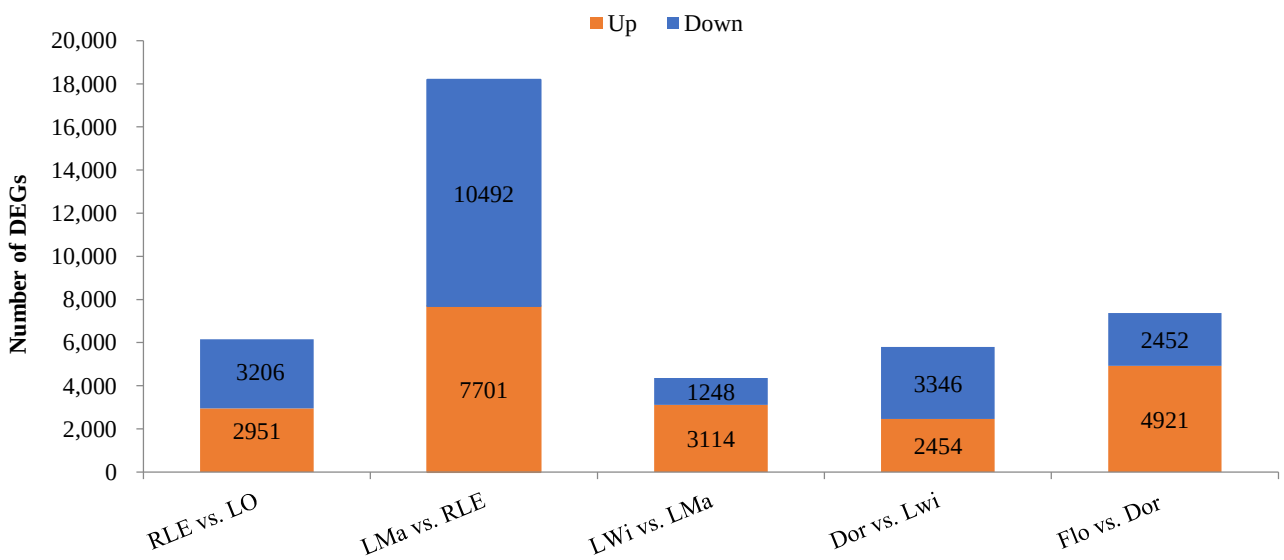

Fig. 1. DEGs identified in the pairwise comparisons of *L. radiata* bulb tips. LO represents the stage of leafing out; RLE represents the stage of rapid leaf extension; LMa represents the stage of leaf maturity; LWi represents the stage of leaf withering; Dor represents the stage of dormancy; and Flo represents the stage of flowering.

For the three stages of reproductive growth (LWi, Dor, and Flo), there were more downregulated GO terms mapped to biological processes in the Dor vs. LWi group, but more upregulated GO terms mapped to biological processes in the Flo vs. Dor group (Table 2). Specifically, biological processes related to stress response were significantly enriched by upregulated DEGs (Fig. 2), and biological processes related to compound biosynthetic and metabolic were significantly enriched by downregulated DEGs in Dor vs. LWi (Fig. 3). The main genes involved in the stress response and heat response are listed in Table 4. Genes encoding heat shock protein 83 exhibited over 64-fold (Log2FC＞6) increased expression in the Dor stage relative to LWi. Furthermore, for Flo vs. Dor, the GO terms enriched by upregulated DEGs were significantly involved in 'organonitrogen compound biosynthetic', 'amide metabolic', and 'biosynthetic processes', etc. (Fig. 2).

KEGG enrichment analysis of the DEGs: KEGG annotation was conducted to further investigate the biological functions of the DEGs. Among the six pairwise comparisons, the DEGs in LMa vs. RLE enriched the most KEGG pathways both at Q value ＜0.05 and p value ＜0.01, followed by Dor vs. LWi and LWi vs. LMa (Fig. 4). However, none of the KEGG pathways enriched by DEGs in RLE vs. LO reached a significant level at a Q value < 0.05 (Fig. 4A). Fig. 5 and Fig. 6 show the top 5 significantly enriched KEGG pathways of upregulated and downregulated DEGs in each pairwise comparison.

Table 2. Number of significantly enriched GO terms (Q value<0.05) in the pairwise comparisons of *Lycoris radiata*.

Pairwise comparisons	Number of up-regulated GO terms			Number of down-regulated GO terms			Total
	BP	CC	MF	BP	CC	MF	
RLE vs. LO	8	4	7	141	80	41	281
LMa vs. RLE	25	5	20	68	34	21	173
LWi vs. LMa	95	40	43	42	27	28	275
Dor vs. Lwi	19	2	31	374	119	200	745
Flo vs. Dor	289	110	105	12	1	16	533

LO represents the stage of leafing out; RLE represents the stage of rapid leaf extension; LMa represents the stage of leaf maturity; LWi represents the stage of leaf withering; Dor represents the stage of dormancy; Flo represents the stage of flowering. BP means biological process, CC means cellular component, and MF means molecular function

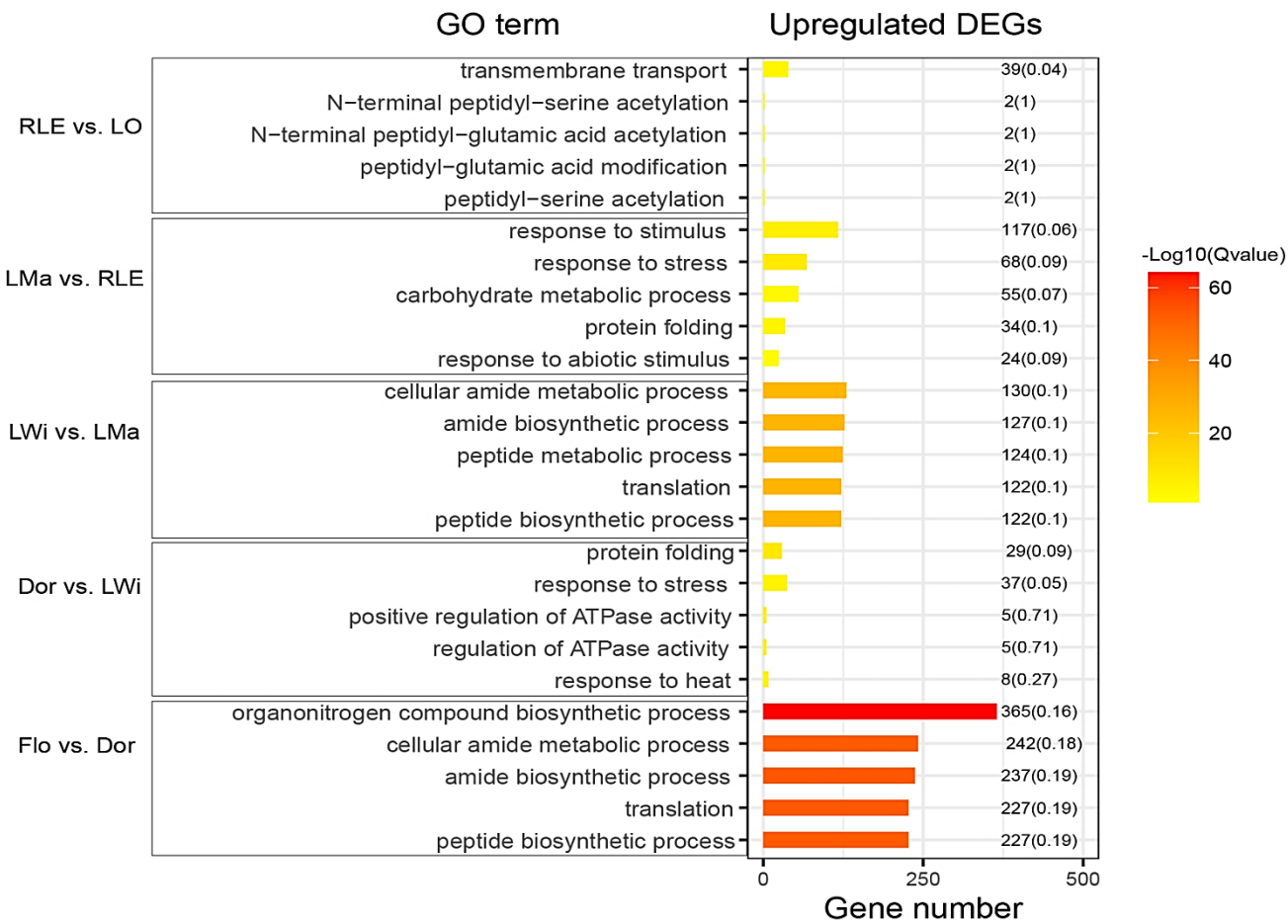

Fig. 2. Top 5 significantly enriched GO terms of the upregulated DEGs in the biological process (BP) category in each pairwise comparison. LO represents the stage of leafing out; RLE represents the stage of rapid leaf extension; LMa represents the stage of leaf maturity; LWi represents the stage of leaf withering; Dor represents the stage of dormancy; and Flo represents the stage of flowering.

WGCNA and gene network analysis: To further study the relationship between gene expression and the development of *L. radiata*, we used WGCNA to divide the identified genes into 19 modules, as shown on the left side of Fig. 7, with each colour representing a module. The Dor stage was highly positively correlated with MElightgreen (r = 0.79) and negatively correlated with MEgrey60 (r = -0.78), indicating that the gene expression in the light green module was upregulated and that in the grey 60 module was downregulated in the Dor stage. Similarly, the Flo stage was positively correlated with Mepurple (r = 0.60), the RLE stage was positively correlated with Meblack (r = 0.74) but negatively correlated with MEtan (r = -0.73), and the LWi stage was positively correlated with MEred (r = 0.71) (Fig. 7).

Furthermore, we selected the top 60 genes by weight from the WGCNA module and constructed the gene network with Cytoscape software. In the gene network, hub genes were in the centre of the regulatory network, with the most connections and highest connectivity. In this paper we found that hub genes annotated as hypothetical proteins (Fig. 8A) in MElightgreen, pyruvate dehydrogenase E1 component subunit beta-like, and dihydrolipoamide dehydrogenase precursor in MEgray60 (Fig. 8B), protein ALP1-like and 60S ribosomal protein L28-1-like in Mepurple (Fig. 8C), ribosomal protein L31e in Meblack (Fig. 8D), 16.0 kDa heat shock protein in MEtan (Fig. 8E), and heat stress transcription Factor C-2a-like in MEred (Fig. 8F). Our results showed that these genes may be involved in the growth and development of *L.* radiata.

Table 3. Parts of upregulated DEGs involved in 'carbohydrate metabolic process' and 'response to abiotic stimulus' by GO enrichment analysis in LMa vs. RLE.

Gene id	log2FC	Carbohydrate metabolic process
		NR_annotation
TRINITY_DN149514_c3_g1	7.67	Glyceraldehyde-3-phosphate dehydrogenase-2C cytosolic [*Gossypium arboreum*]
TRINITY_DN176053_c3_g2	7.34	fructan:fructan 6G-fructosyltransferase [*Allium cepa*]
TRINITY_DN151012_c2_g1	7.26	beta-amylase 8-like protein [*Trifoliumpratense*]
TRINITY_DN160260_c0_g1	6.50	PREDICTED: beta-amylase 1, chloroplastic [*Musa acuminata* subsp. *malaccensis*]
TRINITY_DN142285_c0_g1	5.85	Glycoside hydrolase [*Macleaya cordata*]
TRINITY_DN138929_c1_g7	5.46	PREDICTED: probable cellulose synthase A catalytic subunit 5 [UDP-forming] isoform X3 [*Musa acuminata* subsp. *malaccensis*]
TRINITY_DN151039_c2_g1	5.34	hypothetical protein SORBI_3004G027800 [*Sorghum bicolor*]
TRINITY_DN145659_c1_g1	4.85	fructan:fructan 6G-fructosyltransferase [*Allium cepa*]
TRINITY_DN152159_c0_g2	4.77	hypothetical protein GOBAR_DD19420 [*Gossypium barbadense*]
TRINITY_DN142818_c5_g1	4.73	6-phosphofructo-2-kinase/fructose-2,6-bisphosphatase isoform X2 [*Jatropha curcas*]
		Response to abiotic stimulus
TRINITY_DN139820_c0_g2	6.65	protein ESKIMO 1 [*Asparagus officinalis*]
TRINITY_DN170367_c4_g1	6.38	glyceraldehyde-3-phosphate dehydrogenase GAPA1, chloroplastic isoform X1 [*Capsella rubella*]
TRINITY_DN152331_c3_g2	5.33	HSP20-like chaperones superfamily protein [*Arabidopsisthaliana*]
TRINITY_DN143610_c4_g1	5.18	PREDICTED: chaperone protein ClpB3, chloroplastic isoform X1 [*Elaeisguineensis*]
TRINITY_DN157229_c0_g1	5.13	predicted protein [*Physcomitrella patens*]
TRINITY_DN164944_c5_g2	4.62	PREDICTED: cellulose synthase-like protein D5 [*Elaeisguineensis*]
TRINITY_DN157209_c0_g1	3.45	putative zinc metalloprotease EGY1, chloroplastic [*Ananas comosus*]
TRINITY_DN145355_c2_g2	3.36	hypothetical protein POPTR_001G438900v3 [*Populus trichocarpa*]
TRINITY_DN136466_c0_g1	3.34	PREDICTED: mitochondrial phosphate carrier protein 1, mitochondrial [*Elaeisguineensis*]
TRINITY_DN173323_c3_g1	3.17	LOW QUALITY PROTEIN: cellulose synthase-like protein D5 [*Asparagus officinalis*]

log2FC, log2FoldChange; NR, non-redundant protein sequence database

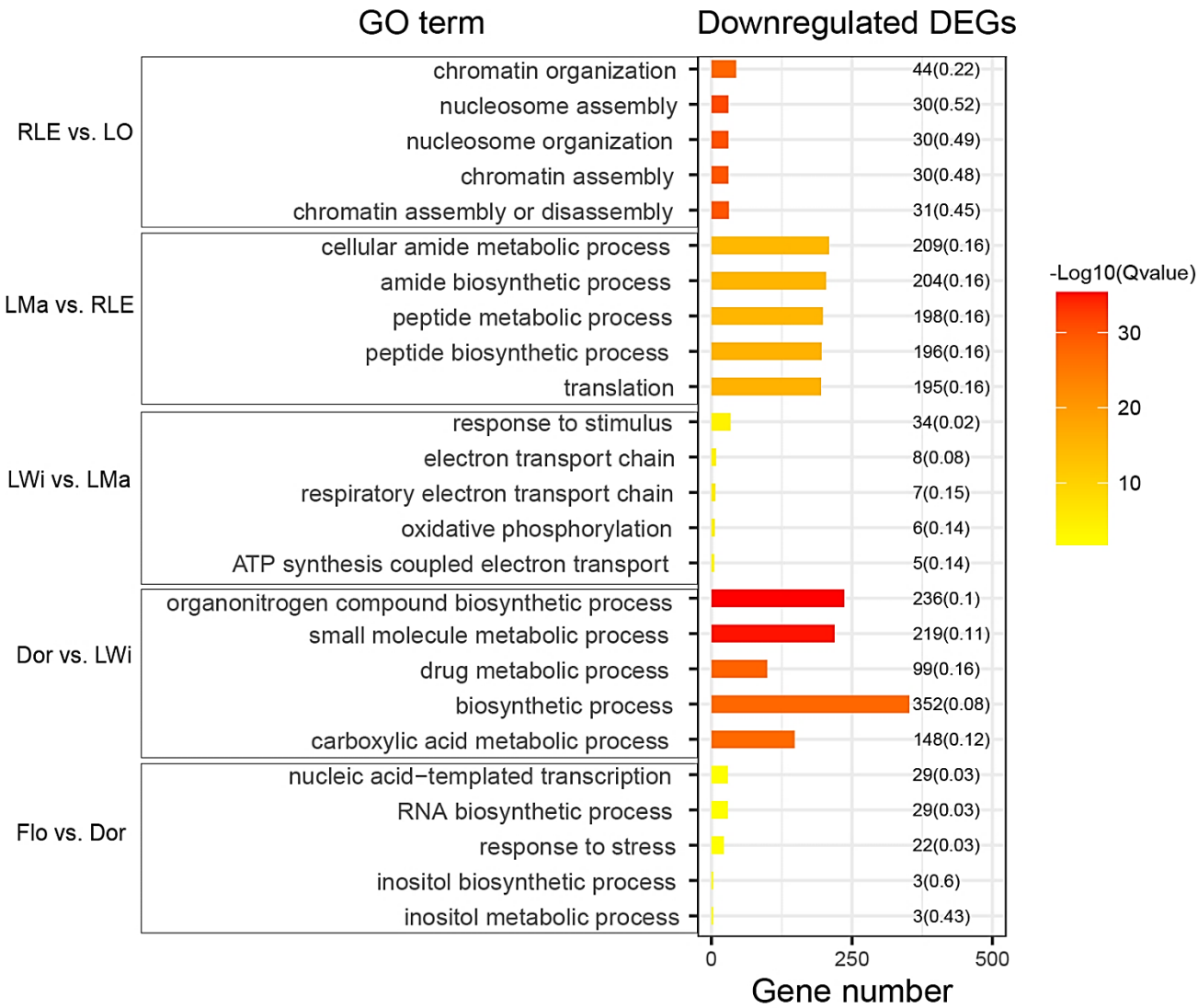

Fig. 3. Top 5 significantly enriched GO terms of the downregulated DEGs in the biological process (BP) category in each pairwise comparison. LO represents the stage of leafing out; RLE represents the stage of ra pid leaf extension; LMa represents the stage of leaf maturity; LWi represents the stage of leaf withering; Dor represents the stage of dormancy; and Flo represents the stage of flowering.

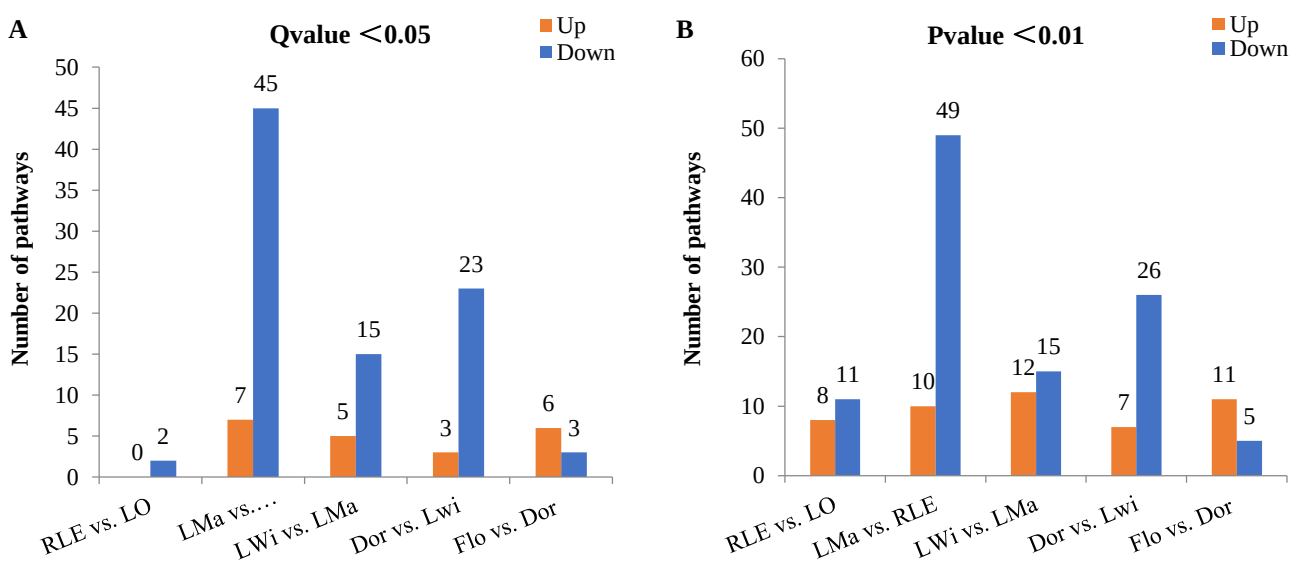

Fig. 4. Number of significantly enriched KEGG pathways at Q value <0.05 (A) and P-value <0.01 (B). LO represents the stage of leafing out; RLE represents the stage of rapid leaf extension; LMa represents the stage of leaf maturity; LWi represents the stage of leaf withering; Dor represents the stage of dormancy; and Flo represents the stage of flowering.

Table 4. The main upregulated DEGs involved in 'response to stress' and 'response to heat' by GO enrichment analysis in Dor vs. LWi.

Gene id	log2FC	Response to stress NR annotation
TRINITY_DN170905_c0_g1	6.72	hypothetical protein GOBAR_AA06605 [*Gossypium barbadense*]
TRINITY_DN172806_c6_g3	6.43	DNA-directed RNA polymerases II, IV and V subunit 9A-like isoform X2 [*Asparagus officinalis*]
TRINITY_DN153753_c1_g1	6.40	heat shock protein 83 [*Cucurbita pepo* subsp. *pepo*]
TRINITY_DN176968_c5_g1	6.37	PREDICTED: heat shock protein 83 [*Populus euphratica*]
TRINITY_DN165008_c1_g1	6.30	PREDICTED: heat shock protein 83 [*Theobroma cacao*]
TRINITY_DN170075_c6_g1	5.35	putative heat shock protein 90, partial [*Ginkgo biloba*]
TRINITY_DN161608_c1_g1	4.13	Thiazole biosynthetic enzyme [*Parasponia andersonii*]
TRINITY_DN168699_c0_g3	3.79	ubiquinol oxidase 2, mitochondrial-like [*Asparagus officinalis*]
TRINITY_DN152331_c3_g2	3.51	PREDICTED: heat shock protein 83-like, partial [*Gossypium hirsutum*]
TRINITY_DN152822_c0_g3	3.49	PREDICTED: chaperone protein ClpB3, chloroplastic isoform X1 [Elaeis guineensis]
		Response to heat
TRINITY_DN165008_c1_g1	3.49	PREDICTED: chaperone protein ClpB3, chloroplastic isoform X1 [*Elaeis guineensis*]
TRINITY_DN170075_c6_g1	2.79	PREDICTED: chaperone protein ClpB3, chloroplastic isoform X1 [*Elaeis guineensis*]
TRINITY_DN143610_c4_g1	2.67	dnaJ protein homolog [*Phalaenopsis equestris*]
TRINITY_DN152331_c3_g2	2.34	hypothetical protein B456_N007500 [*Gossypium raimondii*]
TRINITY_DN152626_c6_g4	2.11	HSP20-like chaperones superfamily protein [*Arabidopsis thaliana*]
TRINITY_DN172462_c1_g2	2.06	dnaJ protein homolog [*Asparagus officinalis*]
TRINITY_DN172462_c1_g4	1.36	PREDICTED: KH domain-containing protein HEN4 [*Phoenix dactylifera*]
TRINITY_DN177200_c1_g2	1.13	RNA-binding KH domain-containing protein RCF3 [*Asparagus officinalis*]

log2FC, log2FoldChange; NR, non-redundant protein sequence database

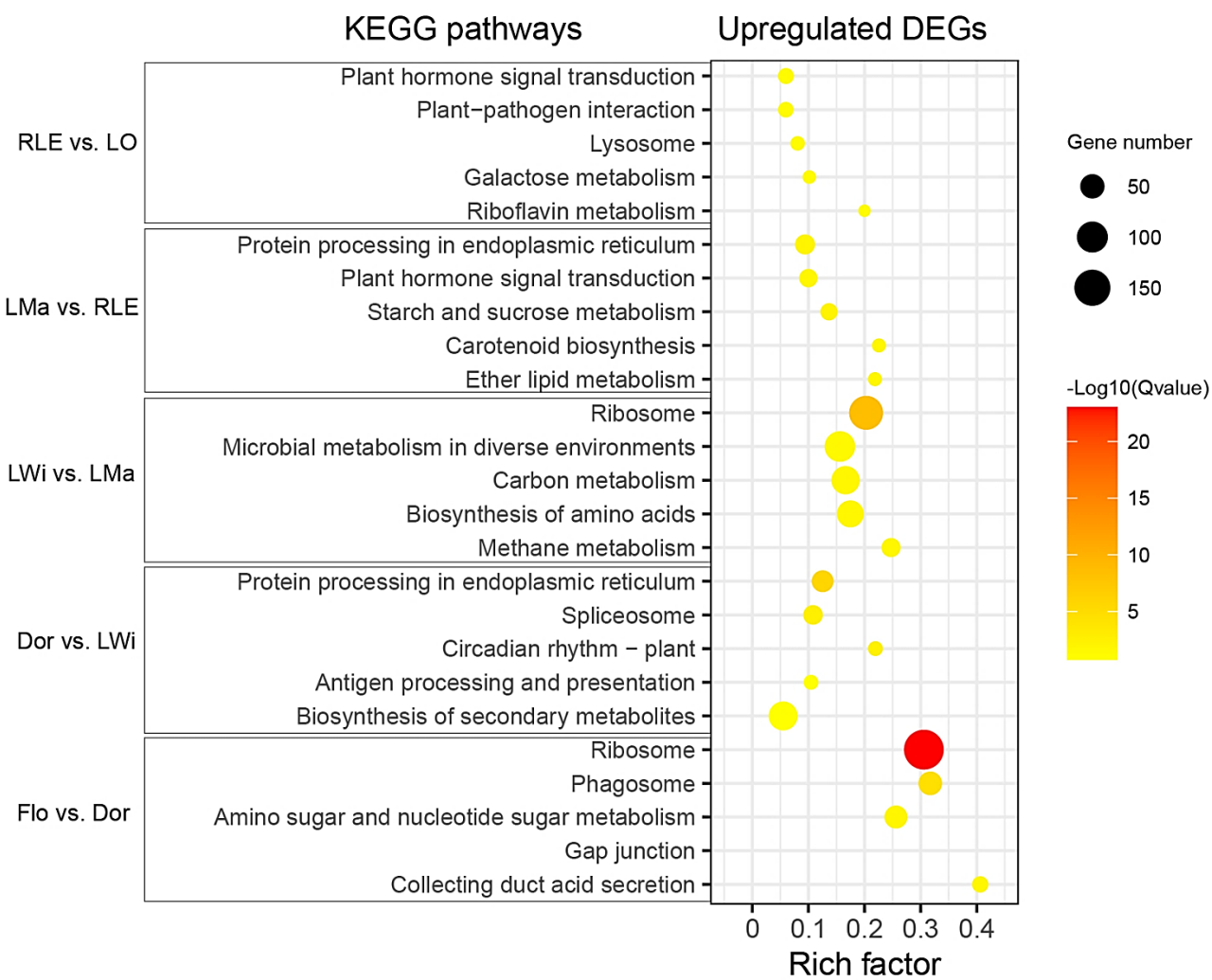

Fig. 5. Top 5 upregulated KEGG pathways in each pairwise comparison. LO represents the stage of leafing out; RLE represents the stage of rapid leaf extension; LMa represents the stage of leaf maturity; LWi represents the stage of leaf withering; Dor represents the stage of dormancy; and Flo represents the stage of flowering.

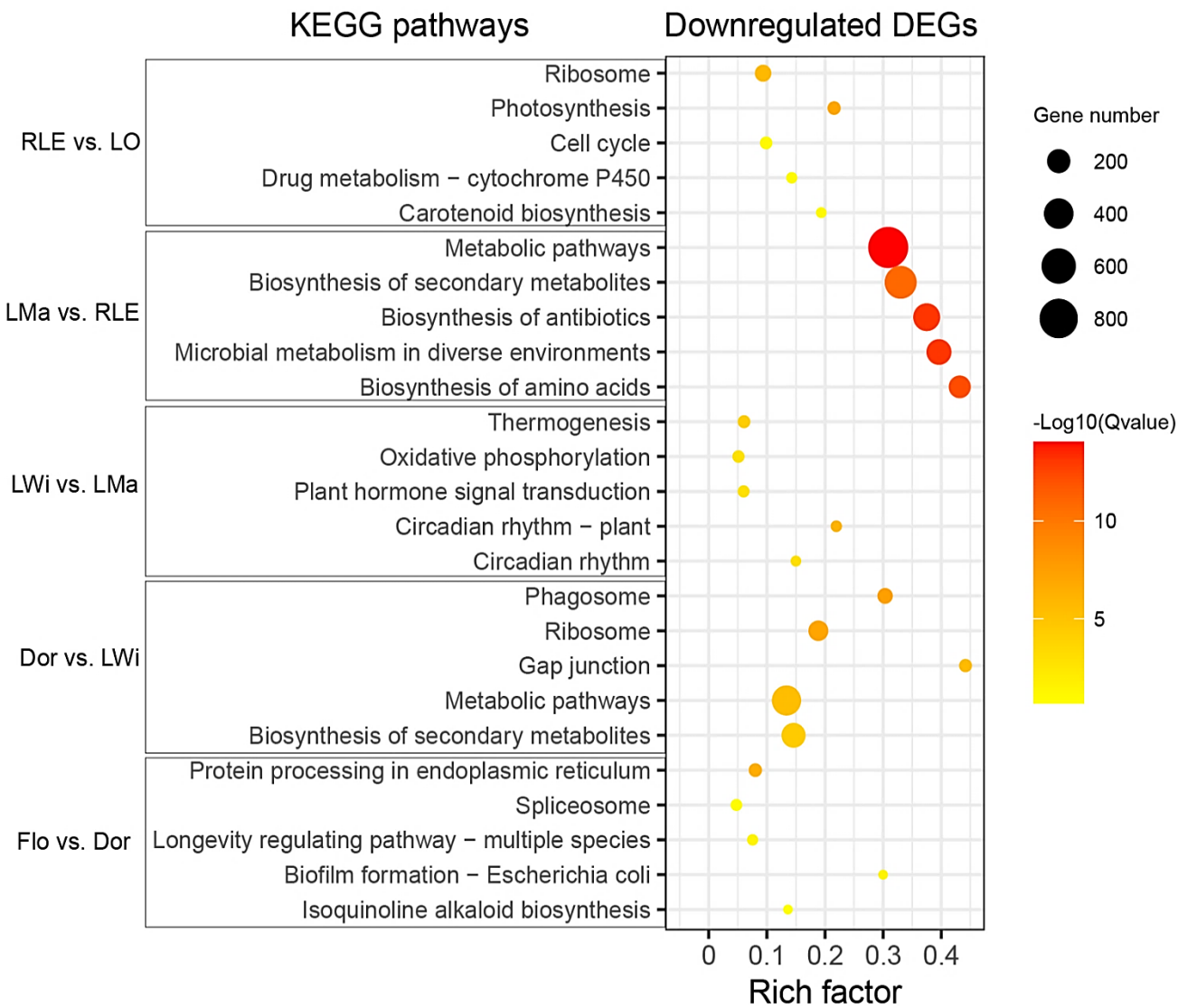

Fig. 6. Top 5 downregulated KEGG pathways in each pairwise comparison. LO represents the stage of leafing out; RLE represents the stage of rapid leaf extension; LMa represents the stage of leaf maturity; LWi represents the stage of leaf withering; Dor represents the stage of dormancy; and Flo represents the stage of flowering.

Discussion

L. radiata shoots out leaves after flowering in fall, goes into dormancy without leaves in summer, and blooms after dormancy, with only scapes appearing above ground (Yang, 2009). However, the molecular mechanisms underlying *L. radiata* development and flowering are poorly understood. In this paper, an RNA-seq approach was used to detect the transcriptome dynamics in the bulb tips of *L. radiata* at six developmental stages (LO, RLE, LMa, LWi, Dor, and Flo). The results showed that an increased number of DEGs were identified with the development of leaves from the LO to LMa stage. The same trend was also observed for leaf senescence and flower bud development from the LWi to Flo stages (Fig. 1).

Carbohydrate metabolism during leaf development: Carbohydrates, which are the main products of photosynthesis in plants, can be divided into structural carbohydrates and nonstructural carbohydrates (NSCs). NSCs include starch and soluble sugars, such as sucrose, glucose, fructose, fructan, etc. (Sakamaki & Ino, 2004). Carbohydrate metabolism comprises a variety of biochemical processes of carbohydrate formation, decomposition, and mutual transformation in organisms. In these processes, energy is provided to cells and tissues in the form of ATP. Starch is the main energy storage substance in plants. A high starch content in bubs is beneficial to flower bud differentiation in *L. aurea* and *L. chinensis* (Zhang *et al*., 2019a). Wu *et al*., (2012) found that starch granules in the cell of the mother scales may serve as a source for growth and development in the *Lilium* Oriental hybrid Sorbonne, and its content showed a significant downwards trend from the shoot emergence stage to the flowering stage. Sucrose is the main form of carbohydrate transported in plants and can regulate plant metabolism at the gene level (Lv *et al*., 2020). Specifically, sucrose may function as a signal molecule to initiate related damage

protection mechanisms and promote the occurrence of bulblets in *L. sprengeri* (Ren *et al*., 2017). In this study, GO and KEGG enrichment analyses showed that the 'carbohydrate metabolic process' (Fig. 2) and 'starch and sucrose metabolism pathway' (Fig. 6) were significantly enriched by upregulated DEGs in LMa vs. RLE. Genes annotated as fructan 6G-fructosyltransferase (6G-FFT), beta-amylase 8 (BAM8)-like protein, and sucrose: sucrose 1-fructosyltransferase were upregulated in LMa relative to RLE (Table 3). Studies have shown that these three genes participate in the metabolism of fructan and starch (Ueno *et al*., 2005; Lasseur *et al*., 2006). Thus, the metabolism of NSCs, including starch, sucrose, and fructan in bulb tips begins to become active during the LMa stage.

Biological process of stress response during leaf development: In this study, the significantly enriched GO terms of 209 upregulated DEGs in LMa vs. RLE were all related to stress response processes, including 'response to abiotic stimulus' (24), 'response to stress' (68), and 'response to stimulus' (117) (Fig. 2). The environmental temperature varies at the LO, RLE, and LMa stages, and the average temperature at LMa is approximately 14℃ lower than that at RLE (Cai *et al*., 2019). Temperature has a great influence on the growth rhythms of *L. radiata*. An appropriate low temperature (9-19°C) and temperature difference between day and night (approximately 9°C) were conducive to the vegetative growth of *L. radiata* (Cai *et al*., 2018b). However, when the temperature was below 5℃, the net photosynthetic rate (PN) decreased significantly, while the initial quantum efficiency (α) increased significantly (Deng *et al*., 2019). These results suggested that the abiotic stress response in *L. radiata* at the LMa stage may be induced by low temperature. This could also be indicated by the upregulation of the encoding protein ESKIMO 1 (Table 3), which is a key gene that plays a crucial role in plant cold acclimation (Xin *et al*., 2007).

Pathway of hormone signal transduction during leaf development: Xu *et al*., (2020a, b) reported that endogenous hormone synthesis and signal transduction were involved in *Lycoris* growth and development. Cytokinin (CK)-, IAA-, and jasmonic acid (JA)-related genes were upregulated in the process of bulb expansion, suggesting that the regulation of IAA, CK, and JA may be positively related to bulb development in *L. radiata*. Wang *et al*., (2020) showed that JA may be involved in the regulation of Amaryllidaceae alkaloids in *L. aurea*. In this study, the KEGG pathway of plant hormone signal transduction was enriched by upregulated DEGs in the RLE vs. LO and LMa vs. RLE comparison groups but enriched by downregulated DEGs in the LWi vs. LMa comparison group (Figs. 5-7). According to a previous study, the LO, RLE, and LMa stages belonged to the vegetative growth period, and the LWi, Dor, and Flo stages belonged to the reproductive growth period (Cai *et al*., 2019). At the LWi stage, flower bud differentiation occurred. These results indicated that genes involved in the hormone signal transduction pathway played a positive role in the regulation of *L. radiat*a leaf growth before flower bud differentiation. Similarly, Zhang *et al*., (2019b) found that before flower bud differentiation, ABA and GA3 levels were higher in the apical meristems of stalks in *Phalaenopsis* cultivars. Zhang *et al*., (2019a) also reported that lower content of IAA, ZR (zeatin riboside), and GA3 in the middle scales of bulbs was beneficial to flower bud differentiation in *L. aurea* and *L. chinensis*.

Pathways and biological process of DEG enrichment during floral differentiation and flowering: Amino acids (AAs) are substrates for protein biosynthesis and are required for the physiological functions of all organisms. Moreover, some amino acids and their metabolites have regulatory effects on gene expression, protein phosphorylation cascade, signal transduction, nitrogen metabolism pathways, and regulation of carbon and nitrogen balance in plants (Wu, 2009). A recent study suggested that amino acid metabolism pathways changed significantly during flower development in *Eriobotrya japonica* (Xu *et al*., 2020b). Our results also showed that genes participating in amino acid biosynthesis were upregulated at the LWi stage (stage of flower bud differentiation) relative to LMa (Fig. 5), suggesting that amino acids of the bulb tips are closely related to flower bud differentiation in *L. radiat*a.

The circadian rhythm enables plants to successfully adapt to environmental stress (Srivastava *et al*., 2019). The circadian clock senses the circadian rhythm of daily environmental factors, such as light, pollinator activities, and temperature, controls plant adaptation to stress, regulates the precise timing of plant flowering, and coordinates with environmental cues to provide assurance of pollination and fertilization (Mora-García, 2017; Jiménez *et al*., 2021). Previous studies suggested that the Dor stage was also the formation stage of the perianth, stamen, and pistil in *L. radiata*, and this stage was very strongly influenced by high ambient temperatures in June and July (Cai, 2012; Cai *et al*., 2019). Indeed, this study found that genes participating in the 'circadian rhythm – plant' pathway were upregulated at the Dor stage relative to LWi (Fig. 5). This may indicate that the development of the perianth, stamen, and pistil is regulated by circadian clock-dependent gating in the temperature sensing pathway. In addition, intercellular signal transduction was highly active at the flowering stage, which is reflected in the significant enrichment of gap junctions by upregulating DEGs in Flo vs. Dor (Fig. 5). Gap junctions are direct channels for communication between cells, allowing small molecules such as inorganic salts, sugars, amino acids, nucleotides, and vitamins to be transferred from one cell's cytoplasm to another to rapidly and reversibly promote the cooperative response of neighbouring cells to external signals (Doerder & Gibson, 2015).

Stage-specific modules and hub genes were identified by using WGNCA. The pyruvate dehydrogenase complex (PDC) is a key metabolic enzyme involved in the TCA cycle (Randall *et al*., 1989). Mitochondrial dihydrolipoamide dehydrogenase is not only involved in the TCA cycle but also a key enzyme involved in life activities such as photorespiration and the degradation of branched-chain α-ketoacids (Lee *et al*., 2019). For example, the dihydrolipoamide dehydrogenase component of the glycine decarboxylase complex was responsible for catalysing the mitochondrial step of photorespiration in pea leaves (Bourguignon *et al*., 1992). In this study, by performing WGNCA, genes encoding pyruvate dehydrogenase E1 component subunit beta-like and dihydrolipoamide dehydrogenase precursor were identified as Dor stage-specific hub genes (Fig. 7, Fig. 8A-B), indicating that the metabolic pathway of the TCA cycle in bulbs of *L. radiat*a was active during the dormancy stage. Ribosomal proteins are the basic component of ribosomes, which are also important for plant growth and stress response (Jin *et al*., 2018). Proteomics research findings showed that 40S ribosomal protein was an important protein identified in the bulb tips of *L. radiata* at the LWi stage (Jiang *et al*., 2021). In the current study, genes encoding ribosomal proteins were identified at both the RLE and Flo stages (Fig. 7, Fig. 8C-D). This suggests that ribosomal proteins may play critical roles in the leaf growth and flowering of *L. radiat*a. The main function of heat stress transcription factors (HSFs) is to regulate the expression of heat shock genes (Li *et al*., 2020). Environmental stress such as heat directly stimulates the activity of HSF, which in turn stimulates the expression of HSP chaperones and affects the expression of reactive oxygen species (ROS) scavenger genes to prevent oxidative damage (Driedonks *et al*., 2015). In this study, genes encoding 16.0 kDa heat shock protein were the hub genes of the MEtan module (Fig. 8E), and there was a significant negative correlation between the MEtan module and RLE (Fig. 7). This result suggested that this gene may play a negative regulatory role in the RLE stage. Heat stress transcription Factor c-2a-like was the hub gene of the MEred module (Fig. 8F), and there was a significant positive correlation between the MEred module and LWi (Fig. 7), indicating that this gene may play a positive regulatory role in the LWi stage.

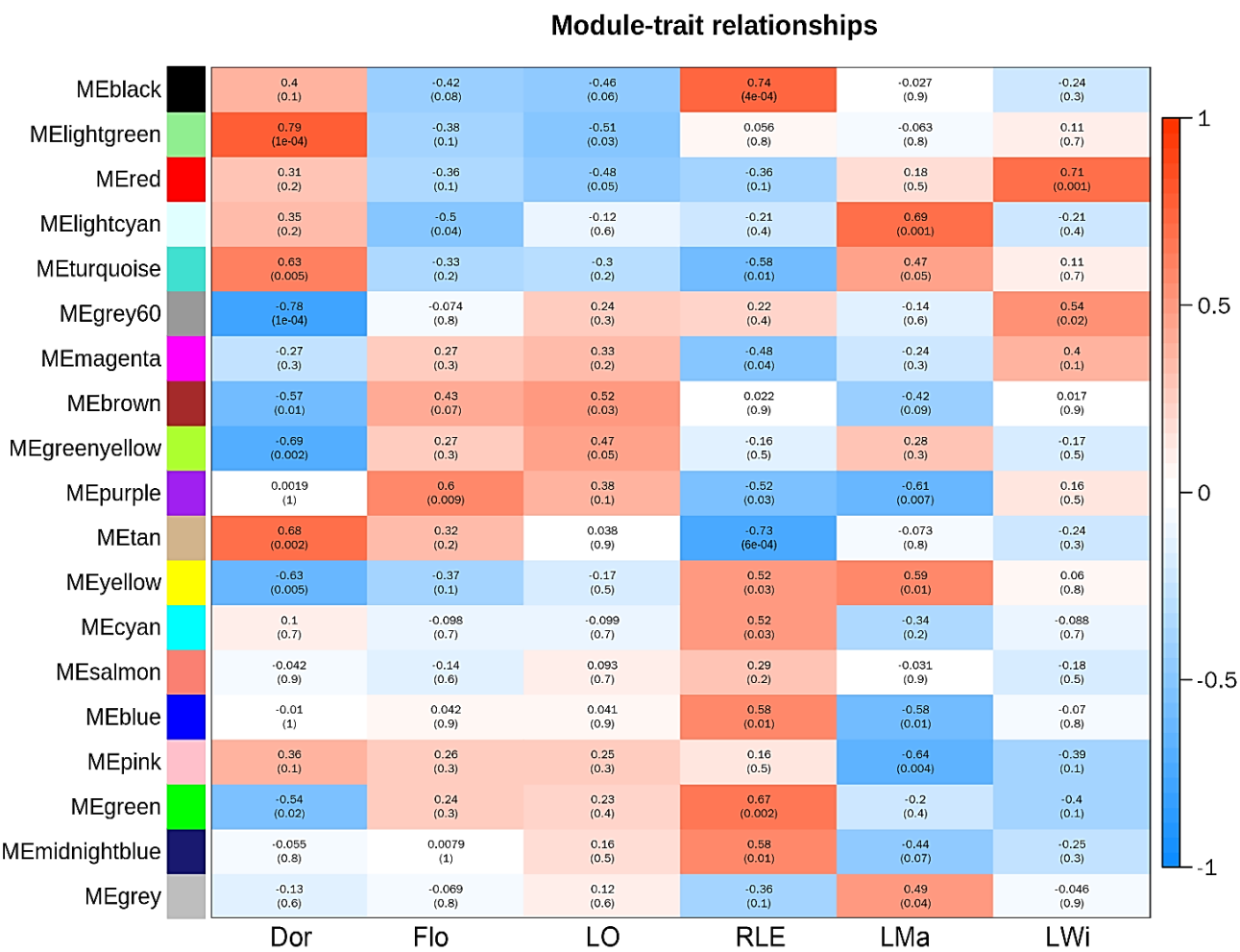

Fig. 7. Analysis of gene association patterns between different stages by WGCNA. The abscissa is the sampling period, the ordinate is the module, and the two numbers on the colour module are the correlation coefficient and P - value (value in parentheses). The colour bar on the right represents the correlation coefficient. The higher the correlation is, the darker the colour, and the lower the correlation is, the lighter the colour. LO represents the stage of leafing out; RLE represents the stage of rapid leaf extension; LMa represents the stage of leaf maturity; LWi represents the stage of leaf withering; Dor represents the stage of dormancy; and Flo represents the stage of flowering.

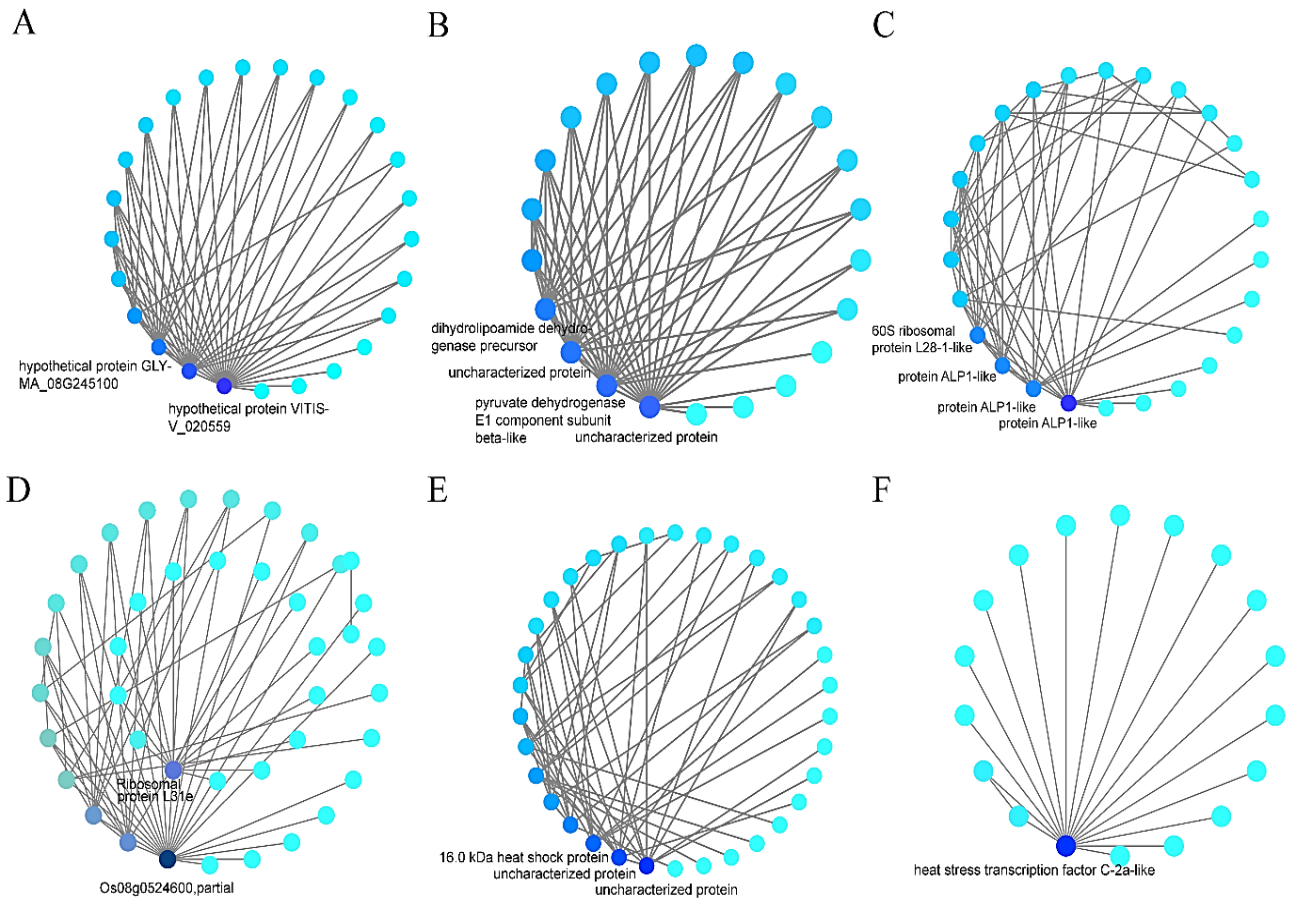

Fig. 8. Gene network in the light green (A), grey 60 (B), purple (C), black (D), tan (E) and red (F) modules. Each node represents a gene, and the connecting line between the nodes means that the two genes have an interaction. The deeper the node is, the more genes that interact with it.

Conclusions

In this study, transcriptomic analyses from the bulb tips of *L. radiata* at six developmental stages were conducted. The KEGG pathways of 'hormone signal transduction', 'starch and sucrose metabolism', and the biological processes of 'carbohydrate metabolism' and 'stress response' were found to be significantly enriched by upregulated DEGs in LMa vs. RLE during leaf development. KEGG pathways of 'biosynthesis of amino acids', 'circadian rhythm - plant' and 'gap junction' were significantly enriched by upregulated DEGs in LWi vs. LMa, Dor vs. LWi, and Flo vs. Dor, respectively, during floral differentiation and flowering. DEGs, such as fructan 6G-fructosyltransferase, beta-amylase 8 (BAM8)-like protein, sucrose: sucrose 1-fructosyltransferase, protein ESKIMO 1, heat stress transcription factors, etc., were screened. These results assist further understanding of the growth and development mechanism of *Lycoris* at the genetic level.

Acknowledgments

This work was supported by the National Natural Science Foundation of China (31960327, 31560226) and Natural Science Foundation of Jiangxi Province (20202BABL205004).

References

Anders, S. and W. Huber. 2012. Differential expression of RNA-Seq data at the gene level-the DESeq package. Heidelberg: European Molecular Biology Laboratory (EMBL).

Benjamini, Y. and Y. Hochberg. 1995. Controlling the false discovery rate: A practical and powerful approach to multiple testing. *J. R. Stat. Soc., Ser. B, Methodol*., 57: 289-300.

Bourguignon, J., D. Macherel, M. Neuburger and R. Douce. 1992. Isolation, characterization, and sequence analysis of a cDNA clone encoding L-protein, the dihydrolipoamide dehydrogenase component of the glycine cleavage system from pea-leaf mitochondria. *Eur. J. Biochem*., 204: 865-873.

Cai, J.H. 2012. Studies on the floral development physiology and key cultivation techniques of cut-flower of *Lycoris radiata*. Ph.D Thesis. Jiangxi Agriculture University, Nanchang. (In Chinese).

Cai, J.H., J.F. Li, X.Y. Wei and L. Zhang. 2018a. Dynamic change in biomass, root vigor and replacement rate during the green leaf period of *Lycoris radiata*. *Journal of Nanjing Forestry University (Natural Sciences Edition)*, 42: 55-59. (In Chinese).

Cai, J.H., J.J. Fan, X.Y. Wei and L. Zhang. 2019. A three-dimensional analysis of summer dormancy in the red spider lily (*Lycoris radiata*). *Hort. Sci*., 54: 1459-1464.

Cai, J.H., J.J. Fan, X.Y. Wei, D.L. Zhang, J.J. Ren and L. Zhang. 2020. Differences in floral development between *Lycoris radiata* and *Lycoris sprengeri*. *Sci. Asia*, 46: 1-9.

Cai, J.H., X.Y. Wei, J.F. Li and L. Zhang. 2018b. The regulation and control of ambient temperature on growth rhythm of *Lycoris radiata*. *Acta Agriculturae Universitatis Jiangxiensis*, 40: 24-31. (In Chinese).

Deng, B., Y.Q. Zhi, Y.H. Zheng, J. Zhou and P.C. Zhang. 2019. Effects of simulated winter and spring temperature changes on photosynthesis of *Lycoris radiata*. *Chinese Agricultural Science Bulletin*, 40: 69-74. (In Chinese).

Doerder, P. and R. Gibson. 2015. General biology. WikiBooks, America.

Driedonks, N., J. Xu, J.L. Peters, S. Park and I. Rieu. 2015. Multi-level interactions between heat shock factors, heat shock proteins, and the redox system regulate acclimation to heat. *Front Plant Sci.*, 6: 999.

Grabherr, M.G., B.J. Haas, M. Yassour, J.Z. Levin, D.A. Thompson, I. Amit, X. Adiconis, L. Fan, R. Raychowdhury, Q. Zeng, Z. Chen, E. Mauceli, N. Hacohen, A. Gnirke, N. Rhind, F. di Palma, B.W. Birren, C. Nusbaum, K. Lindblad-Toh, N. Friedman and A. Regev. 2011. Full-length transcriptome assembly from RNA-Seq data without a reference genome. *Nat. Biotechnol.*, 29: 644-652.

Jiang, X.R., H.T. Chen, X.Y. Wei and J.H. Cai. 2021. Proteomic analysis provides an insight into the molecular mechanism of development and flowering in *Lycoris radiata*. *Acta Physiol. Plant.*, 43: 1.

Jiménez, A., F. Sevilla and M.C. Martí. 2021. Reactive oxygen species homeostasis and circadian rhythms in plants. *J. Exp. Bot.*, 72(16): 5825-5840.

Jin, C.C., M.Y. Hou and Y.Y. Pan. 2018. Research progress of ribosomal protein function in *Arabidopsis thaliana*. *Plant Physiol*., 54(2): 203-212.

Kawano, S. 2009. 13: *Lycoris sanguinea* Maxim. (Amaryllidaceae). *Plant Spec. Biol.*, 24: 139-144.

Langfelder, P. and S. Horvath. 2008. WGCNA: An R package for weighted correlation network analysis. *BMC Bioinform*., 9: 559.

Lasseur, B., J. Lothier, A. Djoumad, B. De Coninck, S. Smeekens, A. Van Laere, A. Morvan-Bertrand, W. Van den Ende and M.P., Prud'homme. 2006. Molecular and functional characterization of a cDNA encoding fructan: fructan 6G-fructosyltransferase (6G-FFT) / fructan: fructan 1-fructosyltransferase (1-FFT) from perennial ryegrass (*Lolium perenne* L.). *J. Exp. Bot.*, 57: 2719-2734.

Lee, H.J., E.J. Park and J.i. Choi. 2019. Isolation, morphological characteristics and proteomic profile analysis of thermo-tolerant *Pyropia yezoensis* mutant in response to high-temperature stress. *Ocean Sci. J*., 54: 65-78.

Li, M., S. Tan, G. Tan, Y. Luo, B. Sun, Y. Zhang, Q. Chen, Y. Wang, F. Zhang, Y.T. Zhang, Y.X. Lin, X.R. Wang and H.R. Tang. 2020. Transcriptome analysis reveals important transcription factor families and reproductive biological processes of flower development in celery *(Apium graveolens* L.). *Agronomy (Basel)*, 10: 653.

Lv, X.S., D. Zhang, R.H. Min, S.Q. Li, Z. Li, Z.M. Ren and Y.P. Xia. 2020. Effects of exogenous sucrose on bulblet formation of *Lycoris sprengeri* in vitro. *Acta Hort. Sin.*, 47: 1475-1489. (In Chinese).

Mao, X., T. Cai, J.G. Olyarchuk and L. Wei. 2005. Automated genome annotation and pathway identification using the KEGG Orthology (KO) as a controlled vocabulary. *Bioinformatics*, 21: 3787-3793.

Mora-García, S., M.J. de Leone and M. Yanovsky. 2017. Time to grow: circadian regulation of growth and metabolism in photosynthetic organisms. *Curr. Opin. Plant Biol*., 35: 84-90.

Park, C.H., H.J. Yeo, Y.E. Park, S. Baek, J.K. Kim and S.U. Park. 2019. Transcriptome analysis and metabolic profiling of *Lycoris radiata*. *Biology*, 8: 63.

Randall, D.D., J.A. Miernyk, T.K. Fang, R.J.A. Budde and K.A. Schuller. 1989. Regulation of the pyruvate dehydrogenase complexes in plants. *Ann. N. Acad. Sci*., 573: 192-205.

Ren, Z., Y. Xia, D. Zhang, Y. Li and Y. Wu. 2017. Cytological analysis of the bulblet initiation and development in *Lycoris* species. *Sci. Hort*., 218: 72-79.

Sakamaki, Y. and Y. Ino. 2004. Response of non- structural carbohydrate content of belowground parts in *Equisetum arvense* according to the irradiance change during a growing season. *J. Plant Res*., 117: 385-391.

Srivastava, D., M. Shamim, M. Kumar, A. Mishra, R. Maurya, D. Sharma, P. Pandey and K.N. Singh. 2019. Role of circadian rhythm in plant system: An update from development to stress response. *Environ Exp Bot*., 162: 256-271.

Ueno, K., S. Onodera, A. Kawakami, M. Yoshida and N. Shiomi. 2005. Molecular characterization and expression of a cDNA encoding fructan: fructan 6G-fructosyltransferase from asparagus (*Asparagus officinalis*). *New Phytol*., 165: 813-824.

Wang, L., Z. Feng, X. Wang, X. Wang and X. Zhang. 2010. DEGseq: An R Package for identifying differentially expressed genes from RNA-seq data. *Bioinformatics*, 26: 136-138.

Wang, P., S. Yu, X. Han, J. Xu, Q. He, S. Xu and R. Wang. 2020. Identification, molecular characterization and expression of JAZ genes in *Lycoris aurea*. *PLoS One*, 15: e230177.

Wang, R.S. 1990. Study on floristic geographical distribution of *Lycoris. Journal of Southwest Forestry University*, 10: 41-48. (In Chinese).

Wu, G. 2009. Amino acids: Metabolism, functions, and nutrition. *Amino Acids*, 37: 1-17.

Wu, S., J. Wu, X. Jiao, Q. Zhang and Y. Lv. 2012. The dynamics of changes in starch and lipid droplets and sub-cellular localization of β-Amylase during the growth of lily bulbs. *J. Integ. Agri*., 11: 585-592.

Xin, Z., A. Mandaokar, J. Chen, R.L. Last and J. Browse. 2007. Arabidopsis ESK1 encodes a novel regulator of freezing tolerance. *Plant J*., 49: 786-799.

Xu, H.X., X.Y. Li and J.W. Chen. 2020b. Studies on the amino acid metabolism and carbohydrate metabolism variation during flower development in *Eriobotrya japonica*. *Acta Hort. Sin.*, 47: 233-241. (In Chinese).

Xu, J., Q. Li, L. Yang, X. Li, Z. Wang and Y. Zhang. 2020a. Changes in carbohydrate metabolism and endogenous hormone regulation during bulblet initiation and development in *Lycoris radiata*. *BMC Plant Biol*., 20: 117-180.

Yang, Z.L. 2009. Genetic diversity and domestication breeding techniques of medicinal *Lycoris radiata*. Ph.D. Thesis. China Academy of Forestry Sciences, Beijing. (In Chinese).

Young, M.D., M.J. Wakefield, G.K. Smyth and A. Oshlack. 2010. Gene ontology analysis for RNA-seq: Accounting for selection bias. *Genom. Biol*., 11: R14.

Zhang, P.C., C.S. Bao and Y. Jiang. 2015. Research advances on the biological characteristics of *Lycoris* and its cultivation techniques. *Subtrop. Plant Sci*., 44: 168-174.

Zhang, Y.J., A. Li, X.Q. Liu, J.X. Sun, W.J. Guo, J.W. Zhang and Y.M. Lyu. 2019b. Changes in the morphology of the bud meristem and the levels of endogenous hormones after low temperature treatment of different *Phalaenopsis* cultivars. *S. Afr. J. Bot*., 125: 499-504.

Zhang, Y.T., X.L. Yang, L. He and L.G. Wang. 2019a. Relationships between flower bud differentiation in two kinds of *Lycoris* and the changes of carbohydrate, antioxidant enzymes and endogenous hormones. *J. Anhui Agri. Uni.*, 46: 342-349. (In Chinese).

(Received for publication 27 September 2021)